

# ORBITAL EVOLUTION OF GEOSYNCHRONOUS OBJECTS WITH HIGH AREA-TO-MASS RATIOS

Luciano Anselmo and Carmen Pardini

ISTI/CNR, Area della Ricerca di Pisa, Via Moruzzi 1, 56124 Pisa, Italy  
Email: Luciano.Anselmo@isti.cnr.it, Carmen.Pardini@isti.cnr.it

## ABSTRACT

The dynamical evolution of objects released in geostationary orbit with area-to-mass ratios ( $A/M$ ) between 1 and  $50 \text{ m}^2/\text{kg}$  was analyzed, both short (a few months) and long-term (54 years), taking into account geopotential harmonics ( $8 \times 8$ ), luni-solar perturbations, direct solar radiation pressure with eclipses and, when applicable, air drag. The results obtained confirm that such objects may be good candidates to explain the recently discovered debris population with mean motions of about one revolution per day and orbital eccentricities as high as 0.55.

More specifically, for  $A/M > 40 \text{ m}^2/\text{kg}$ , orbital decay is attained in less than 40 months due to the eccentricity rise, while, for lower values of the area-to-mass ratio, a lifetime of at least two decades was found. Increasing  $A/M$  from 1 to  $15 \text{ m}^2/\text{kg}$ , the amplitude of the short-term eccentricity oscillation grows from about 0.03 to 0.3, while the long-term variation increases from approximately 0.02 to 0.5. Above  $15 \text{ m}^2/\text{kg}$ , the pattern of eccentricity evolution becomes more complicated, with typically larger excursions. Concerning the inclination evolution, objects with  $A/M = 1 \text{ m}^2/\text{kg}$  exhibit the classical behavior of a typical abandoned geostationary spacecraft. However, a further increase of the area-to-mass ratio has as consequence a faster orbit pole precession and wider amplitude of the plane motion.

## 1. INTRODUCTION

Optical observations have discovered a substantial amount of decimeter sized objects in orbits close to the geosynchronous altitude (Flury et al., 2000; Schildknecht et al., 2001; 2002; 2004a). Most of these are probably the result of a still undetermined number of explosions occurred to spacecraft and upper stages. So far, however, only two fragmentations have been confirmed near the geostationary orbit (Johnson et al., 2004) and the identification of further explosions at a so high altitude is complicated by the long time passed since the occurrence of the events and by the effects of the orbital perturbations on the resulting debris clouds (Pardini and Anselmo, 2003).

Recent observations, carried out by the ESA's 1 m

telescope in Tenerife, have identified an additional population of faint uncatalogued objects, with mean motions of about 1 revolution per day and orbital eccentricities as high as 0.55 (Schildknecht et al., 2004b). The discovery of such objects was quite surprising, but an obvious explanation for their origin was immediately proposed. In fact, the direct solar radiation pressure may significantly affect the eccentricity with small effects on the total energy of the orbit and, therefore, on the semimajor axis or mean motion. However, this perturbation is adequately effective only on objects with sufficiently high area-to-mass ratios (Liou and Weaver, 2004).

## 2. SIMULATIONS DESCRIPTION

In order to understand the possible origin of the above mentioned nearly geosynchronous population in eccentric orbit, the dynamical evolution of objects with area-to-mass ratios between 1 and  $50 \text{ m}^2/\text{kg}$  was analyzed, both short (a few months) and long-term (54 years). The simulations were carried out by releasing in geostationary orbit test objects with area-to-mass ratios in the above mentioned range and a negligible velocity variation ( $\Delta V$ ). The chosen release orbits and longitudes corresponded to those of controlled operational satellites close to the stable and unstable equilibrium points of the geopotential, plus a fifth intermediate longitude (see Tab. 1).

*Table 1. Initial conditions (beginning of 2005) used in the simulations in terms of semimajor axis ( $a$ ), eccentricity ( $e$ ), inclination ( $i$ ) and longitude East ( $\lambda$ ). Two longitudes were near the stable equilibrium points of the geopotential (S1 and S2), other two were close to the unstable equilibrium points (U1 and U2) and a fifth was at  $\cong 45 \text{ deg}$  from the first stable and unstable points (L1).*

Initial Conditions	$a$ [km]	$e$	$i$ [deg]	$\lambda$ [deg]
S1	42165.9	0.00026	0.0538	74.94
L1	42167.2	0.00014	0.0656	119.95
U1	42166.0	0.00023	0.0293	166.00
S2	42166.2	0.00034	0.0192	254.97
U2	42166.0	0.00023	0.0161	344.99

The latter choice was motivated by the need to consider the broadest set of geopotential initial conditions, while maintaining, at the same time, the number of simulations at a minimum. Concerning the use of parent satellites station-kept both in longitude and inclination, the choice adopted – considered a starting point – was dictated by the need to simplify the analysis of the results in what is considered a preliminary approach to the topic.

The simulated objects were numerically propagated for 54 years (a time span approximately close to the well known precession period of the orbital plane of an abandoned geostationary spacecraft) with a special perturbations software (Pardini and Anselmo, 1994; Kwok, 1987), taking into account geopotential harmonics, up to the eight degree and order, luni-solar attraction and direct solar radiation pressure, including the eclipses due to the Earth’s shadow. In case of high eccentricity orbits with perigee altitude below 1000 km, the perturbing effects of the air drag were considered as well, adopting the 1976 United States Standard Atmosphere.

### 3. SHORT-TERM ORBITAL EVOLUTION

The short-term orbital evolution ( $\leq 1$  year) is qualitatively similar in all the cases analyzed and is exemplified in Figs. 1 and 2, for objects released in S2 (but the same applies to S1, U1 and U2 as well), and in Figs. 3 and 4, for objects released in L1 (see Tab. 1). There is a rapid growth of both mean eccentricity and inclination, strongly correlated with the area-to-mass ratio (A/M): the greater the latter, the larger the effect. For objects above a certain A/M threshold (40  $\text{m}^2/\text{kg}$  for those released in the equilibrium points, 44  $\text{m}^2/\text{kg}$  for those released in L1), the eccentricity becomes so large, and the perigee so low, that a decay from orbit in less than six months is induced.

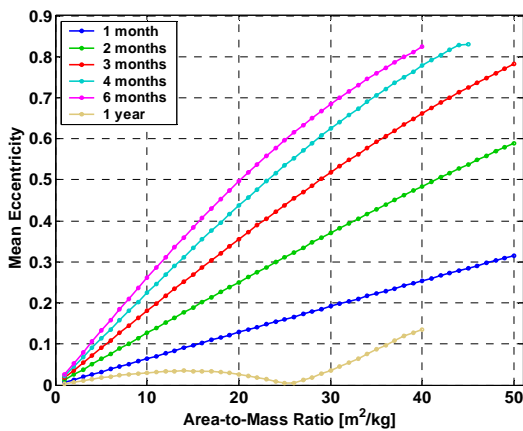


Figure 1. Short-term mean eccentricity evolution as a function of the area-to-mass ratio (S2 case).

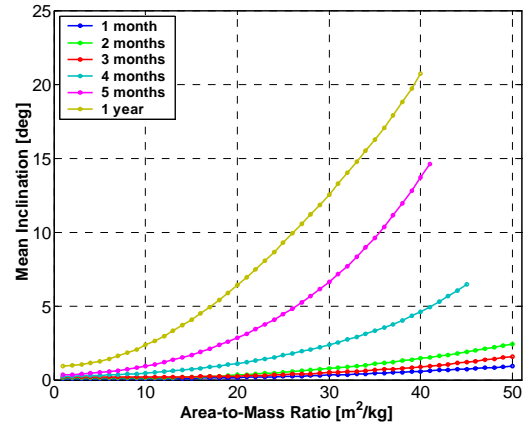


Figure 2. Short-term mean inclination evolution as a function of the area-to-mass ratio (S2 case).

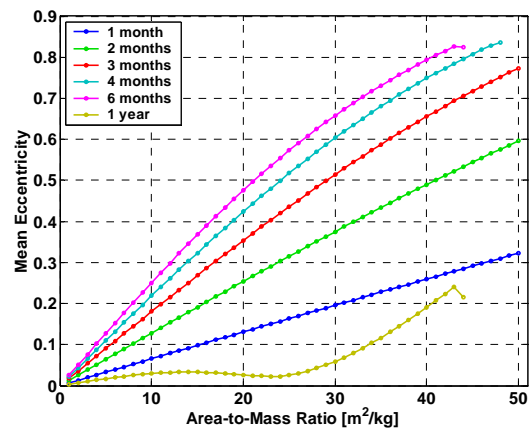


Figure 3. Short-term mean eccentricity evolution as a function of the area-to-mass ratio (L1 case).

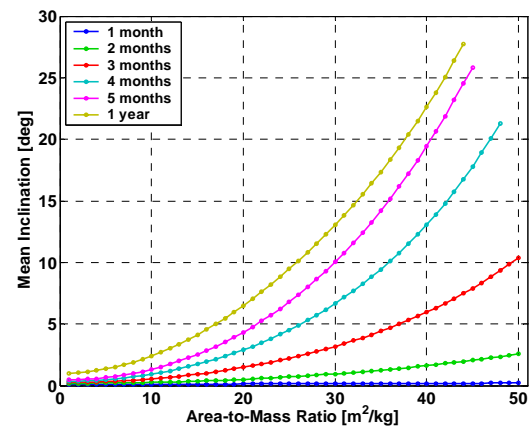


Figure 4. Short-term mean inclination evolution as a function of the area-to-mass ratio (L1 case).

The objects with A/M below such a threshold escape this fate and after six months their eccentricity inverts the trend, reaching a new minimum approximately one year after the beginning of the simulations (Figs. 1 and

3). The semimajor axis remains in these cases close to the geosynchronous one (Fig. 5), while the inclination continues to grow (Figs. 2 and 4).

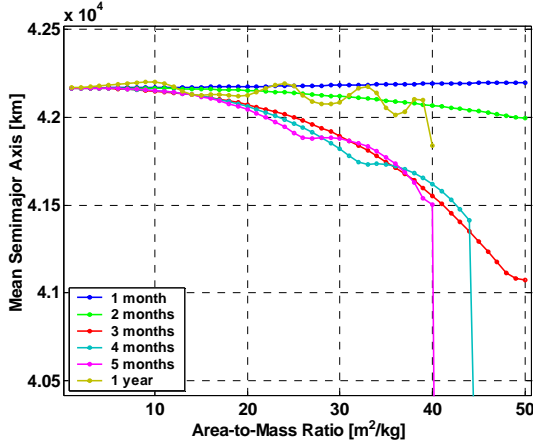


Figure 5. Short-term mean semimajor axis evolution as a function of the area-to-mass ratio (S2 case).

#### 4. LONG-TERM ORBITAL EVOLUTION

Also the long-term orbital evolution is a function of the area-to-mass ratio, even though the outcome is not always obvious. For example, in general the objects with  $A/M$  up to  $35 \text{ m}^2/\text{kg}$  are still in orbit after 54 years (the upper limit of the simulations), with a semimajor axis close to the geosynchronous one, independently of the initial conditions. However, there are intermediate values of the area-to-mass ratios ( $16\text{-}17 \text{ m}^2/\text{kg}$ , for the objects released in the equilibrium points;  $16\text{-}20 \text{ m}^2/\text{kg}$ , for the objects released in L1) for which a significantly shorter orbital lifetime is expected, in between 29 and 41 years (Fig. 6).

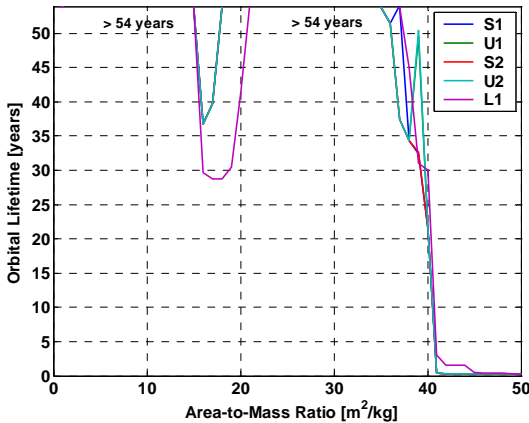


Figure 6. Orbital lifetime as a function of the area-to-mass ratio and initial release conditions.

For  $A/M > 35 \text{ m}^2/\text{kg}$ , the lifetime typically decreases with higher values of the area-to-mass ratio, even if in certain cases (S1 for  $A/M = 37 \text{ m}^2/\text{kg}$ , U1 and U2 for

$A/M = 39 \text{ m}^2/\text{kg}$ ) this trend may be locally violated. In any case, all the objects with  $A/M > 40 \text{ m}^2/\text{kg}$ , including those released in L1, decay from orbit in less than 40 months, while for  $35 \text{ m}^2/\text{kg} < A/M \leq 40 \text{ m}^2/\text{kg}$  the orbital lifetime is greater than 21 years, the exact value depending on the area-to-mass ratio and initial conditions.

During the time span considered (54 years), the orbital behavior of the objects with  $A/M \leq 35 \text{ m}^2/\text{kg}$  released near the equilibrium points of the geopotential, both stable and unstable, is very similar. As a matter of fact, the long-term evolution of eccentricity and inclination matches so well that the plots for a single case, for instance S2, can be used as accurate representations of the other cases S1, U1 and U2. For L1 the details of the evolution are different, but the general pattern is comparable.

The long-term eccentricity evolution is plotted in Figs. 7-9 for S2 (or, equivalently, for S1, U1 and U2) and in Figs. 10-12 for L1. For clarity, only a subset of area-to-mass ratios, between 1 and  $40 \text{ m}^2/\text{kg}$ , is shown. In addition to the yearly eccentricity oscillation, evident in all the plots, some long-term trends are recognizable. Increasing  $A/M$  from 1 to  $15 \text{ m}^2/\text{kg}$ , the amplitude of the short-term oscillation, with a period of nearly one year, significantly grows, from  $\sim 0.03$  to  $\sim 0.3$  (Figs. 7, 8, 10 and 11). The same applies to the long-term oscillation: for  $A/M = 1 \text{ m}^2/\text{kg}$  the amplitude is  $\sim 0.02$ , while for  $A/M = 15 \text{ m}^2/\text{kg}$  the amplitude becomes  $\sim 0.5$  (Figs. 7, 8, 10 and 11). However, the oscillation period, 45-50 years for  $A/M = 1 \text{ m}^2/\text{kg}$  (Figs. 7 and 10), increases with larger area-to-mass ratios, reaching 64-74 years for  $A/M = 15 \text{ m}^2/\text{kg}$  (Figs. 8 and 11).

For area-to-mass ratios above  $15 \text{ m}^2/\text{kg}$ , there is a range of values ( $16\text{-}17 \text{ m}^2/\text{kg}$  with S1, U1, S2 and U2,  $16\text{-}20 \text{ m}^2/\text{kg}$  with L1) for which the short and long-term oscillations combine in a way to produce a so large eccentricity able to induce orbital decay (see, for example, the L1 case with  $A/M = 20 \text{ m}^2/\text{kg}$  in Fig. 11). For larger  $A/M$  values (up to  $\sim 25 \text{ m}^2/\text{kg}$ , depending on the initial conditions), the maximum eccentricity comes back to safer values ( $< 0.6\text{-}0.7$ ), but the evolution presents a more complicated pattern (Figs. 8 and 11). From  $25$  to  $40 \text{ m}^2/\text{kg}$  the eccentricity evolution shows the characteristic signature of beats, whose maximum amplitude and frequency increase along with the area-to-mass ratio (Figs. 8, 9, 11 and 12). At  $40 \text{ m}^2/\text{kg}$  the amplitude of the eccentricity oscillation is so large to induce an earlier orbital decay (Figs. 9 and 12).

Concerning the long-term evolution of the inclination, the results are summarized in Figs. 13 and 14 for S2 (or, equivalently, for S1, U1 and U2) and in Figs. 15 and 16 for L1. The objects with  $A/M = 1 \text{ m}^2/\text{kg}$  display the

classical behavior of a typical abandoned geostationary spacecraft, with a maximum inclination of 15 deg and a periodicity of about 53 years (Figs. 13 and 15).

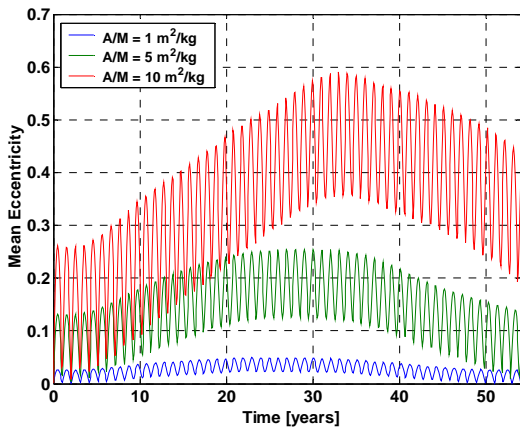


Figure 7. Long-term mean eccentricity evolution for area-to-mass ratios of 1, 5 and 10 m<sup>2</sup>/kg (S2 case).

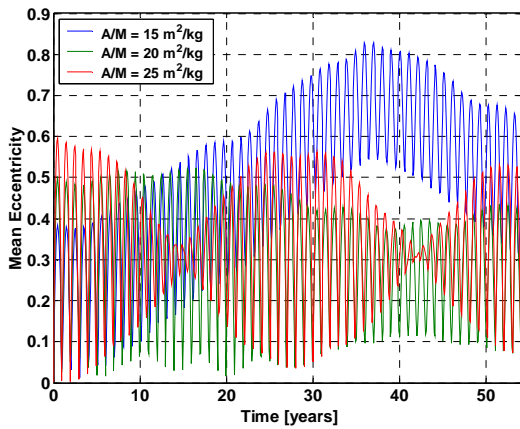


Figure 8. Long-term mean eccentricity evolution for area-to-mass ratios of 15, 20 and 25 m<sup>2</sup>/kg (S2 case).

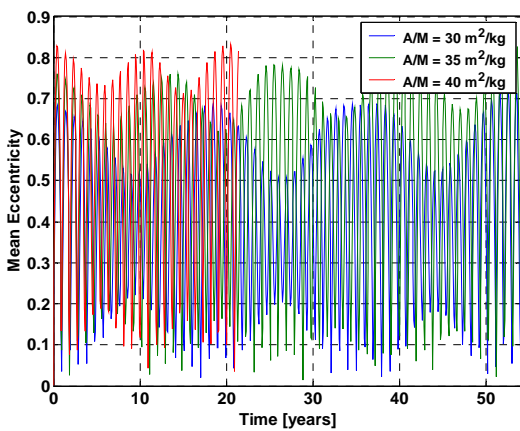


Figure 9. Long-term mean eccentricity evolution for area-to-mass ratios of 30, 35 and 40 m<sup>2</sup>/kg (S2 case).

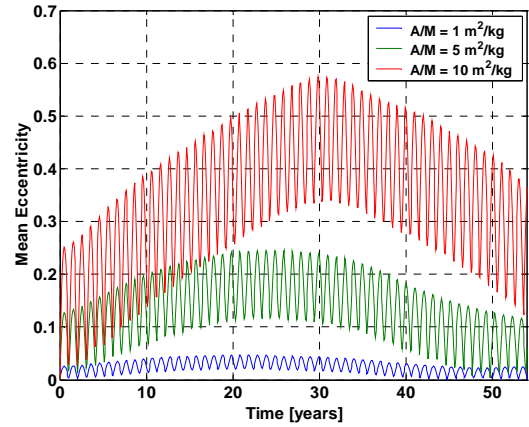


Figure 10. Long-term mean eccentricity evolution for area-to-mass ratios of 1, 5 and 10 m<sup>2</sup>/kg (L1 case).

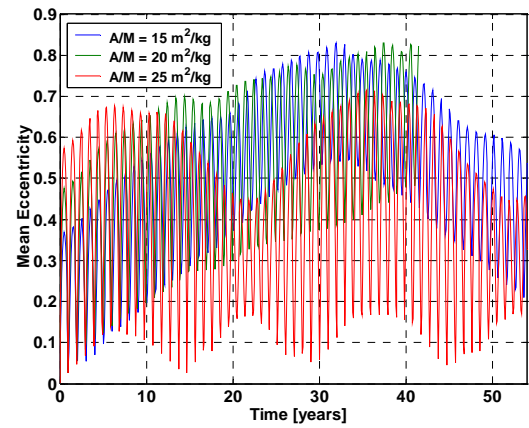


Figure 11. Long-term mean eccentricity evolution for area-to-mass ratios of 15, 20 and 25 m<sup>2</sup>/kg (L1 case).

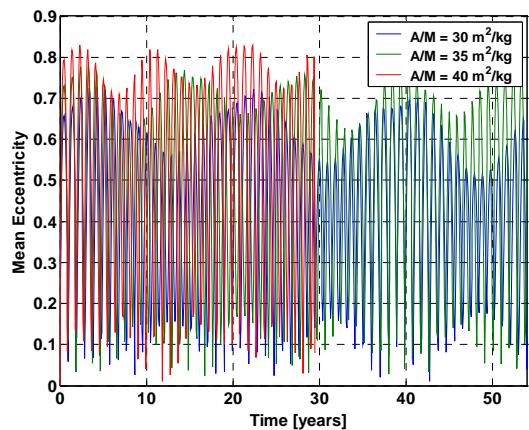


Figure 12. Long-term mean eccentricity evolution for area-to-mass ratios of 30, 35 and 40 m<sup>2</sup>/kg (L1 case).

An increase of the area-to-mass ratio has as consequence a faster orbit pole precession and wider amplitude of the plane motion. For example, objects with A/M = 10 m<sup>2</sup>/kg may reach orbital inclinations



close to 25 deg during cycles of approximately 30 years, while for  $A/M = 40 \text{ m}^2/\text{kg}$  the maximum inclination is  $\sim 45\text{-}50$  deg, with a periodicity of about 5.6 years.

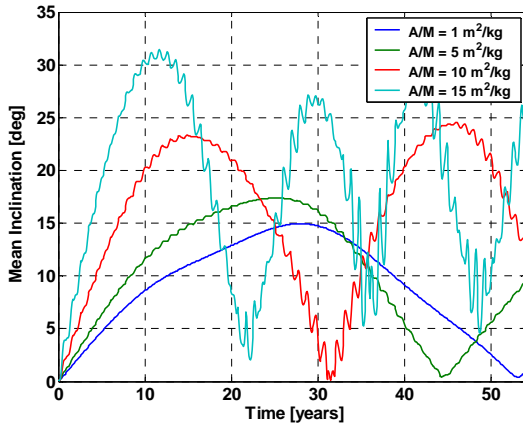


Figure 13. Long-term mean inclination evolution for area-to-mass ratios of 1, 5, 10 and 15  $\text{m}^2/\text{kg}$  (S2 case).

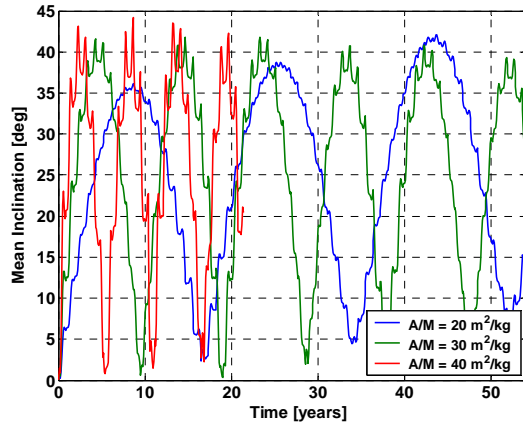


Figure 14. Long-term mean inclination evolution for area-to-mass ratios of 20, 30 and 40  $\text{m}^2/\text{kg}$  (S2 case).

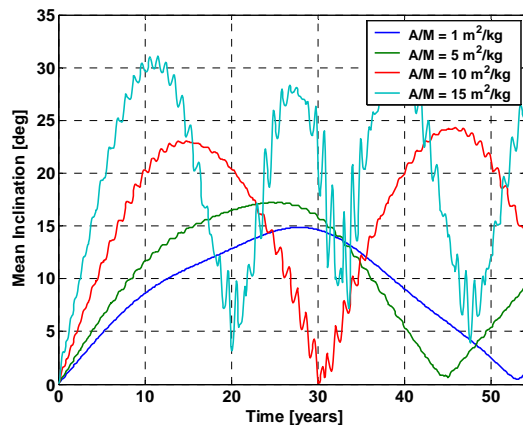


Figure 15. Long-term mean inclination evolution for area-to-mass ratios of 1, 5, 10 and 15  $\text{m}^2/\text{kg}$  (L1 case).

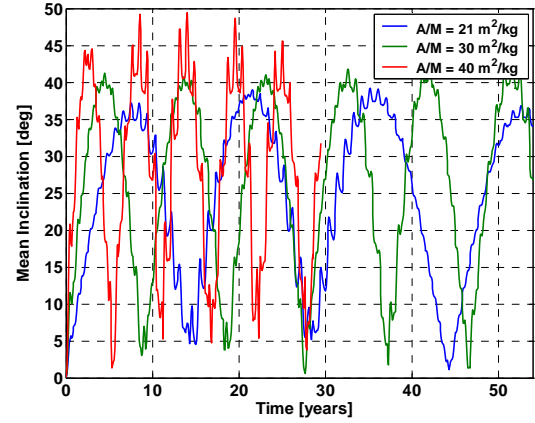


Figure 16. Long-term mean inclination evolution for area-to-mass ratios of 21, 30 and 40  $\text{m}^2/\text{kg}$  (L1 case).

## 5. CONCLUSIONS

The results obtained confirm that objects with high area-to-mass ratios released in geostationary orbit with a negligible  $\Delta V$  may explain the recently discovered debris population with mean motions of about 1 revolution per day and orbital eccentricities as high as 0.55 (Schildknecht et al., 2004b). However, the detailed simulations carried out, in which the dynamical evolution of objects with area-to-mass ratios between 1 and 50  $\text{m}^2/\text{kg}$  was analyzed, both short (a few months) and long-term (54 years), revealed a quite rich collection of behaviors, potentially able to shed light on the debris origin and history when more complete observational data will be available.

Among the main results obtained there are the following, arranged in terms of the effects on orbital lifetime, semimajor axis, eccentricity and inclination:

### Orbital Lifetime and Semimajor Axis

- For objects above a certain  $A/M$  threshold (40-44  $\text{m}^2/\text{kg}$ , depending on the initial conditions), the eccentricity becomes so large, and the perigee so low, that a decay from orbit in less than six months is induced;
- All the objects with  $A/M > 40 \text{ m}^2/\text{kg}$  decay from orbit in less than 40 months;
- In general the objects with  $A/M$  up to 35  $\text{m}^2/\text{kg}$  are still in orbit after 54 years, with a semimajor axis close to the geosynchronous one;
- There are intermediate values of the area-to-mass ratios ( $\sim 16\text{-}20 \text{ m}^2/\text{kg}$ ) for which a significantly shorter orbital lifetime is expected (29-41 years);
- For  $35 \text{ m}^2/\text{kg} < A/M \leq 40 \text{ m}^2/\text{kg}$  the orbital lifetime is greater than 21 years, the exact value depending on the area-to-mass ratio and initial conditions;

- Being the orbital decay typically induced by an eccentricity growth and a sudden decrease of the perigee height, the semimajor axis and the orbital period remain close to the geosynchronous ones until the actual reentry;

### Eccentricity

- Increasing A/M from 1 to 15 m<sup>2</sup>/kg, the amplitude of the short-term eccentricity oscillation, with a period of nearly one year, grows from ~ 0.03 to ~ 0.3;
- Increasing A/M from 1 to 15 m<sup>2</sup>/kg, the amplitude of the long-term eccentricity oscillation grows from ~ 0.02 to ~ 0.5, along with the oscillation period;
- For area-to-mass ratios above 15 m<sup>2</sup>/kg, there is a range of values (~ 16-20 m<sup>2</sup>/kg) for which the short and long-term oscillations combine in a way to produce a so large eccentricity able to induce orbital decay;
- For larger A/M values (up to ~ 25 m<sup>2</sup>/kg, depending on the initial conditions) the maximum eccentricity comes back to safer values (< 0.6-0.7);
- From 25 to 40 m<sup>2</sup>/kg the eccentricity evolution shows the characteristic signature of beats, whose maximum amplitude and frequency increase along with the area-to-mass ratio;
- At 40 m<sup>2</sup>/kg the amplitude of the eccentricity oscillation is so large to induce an earlier orbital decay;

### Inclination

- The objects with A/M = 1 m<sup>2</sup>/kg display the classical behavior of a typical abandoned geostationary spacecraft, with a maximum inclination of 15 deg and a periodicity of about 53 years;
- An increase of the area-to-mass ratio has as consequence a faster orbit pole precession and wider amplitude of the plane motion;
- For objects with A/M = 40 m<sup>2</sup>/kg the maximum inclination is ~ 45-50 deg, with a periodicity of about 5.6 years.

The chosen release orbits and longitudes corresponded to those of controlled operational satellites close to the stable and unstable equilibrium points of the geopotential, plus a fifth intermediate longitude (see Tab. 1). This means that the parent spacecraft were controlled both in longitude and inclination (East-West and North-South station-keeping). In addition, a Sun-pointing perigee strategy was adopted to control the small operational eccentricity.

Concerning the lunar third body perturbation, the right ascension of the ascending node of the Moon at the initial epoch of the simulations (beginning of 2005) was

about 5 deg. Further work is currently on-going to confirm the applicability of the results obtained to a wider set of initial conditions in geostationary orbit.

## 6. REFERENCES

- Flury W., et al., Searching for Small Debris in Geostationary Ring – Discoveries with the Zeiss 1-metre Telescope, *ESA Bulletin*, Vol. 104, 92-100, 2000.
- Johnson N.L., et al., *History of On-Orbit Satellite Fragmentations*, 13<sup>th</sup> Edition, Orbital Debris Program Office, JSC 62530, Johnson Space Center, NASA, Houston, Texas, USA, pp. 11-22, May 2004.
- Kwok J.H., *The Artificial Satellite Analysis Program (ASAP)*, Version 2.0, JPL NPO-17522, Jet Propulsion Laboratory (JPL), Pasadena, California, USA, April 20, 1987.
- Liou J.-C. and Weaver J.K., Orbital Evolution of GEO Debris with Very High Area-to-Mass Ratios, *The Orbital Debris Quarterly News*, Vol. 8, Issue 3, 6-7, July 2004.
- Pardini C. and Anselmo L., *SATRAP: Satellite Reentry Analysis Program*, Internal Report C94-17, CNUCE Institute, Consiglio Nazionale delle Ricerche (CNR), Pisa, Italy, August 30, 1994.
- Pardini C. and Anselmo L., Long-Term Evolution of Debris Clouds in Geosynchronous Orbit, in *Proceedings of the 17<sup>th</sup> International Symposium on Space Flight Dynamics*, held in Moscow, Russia, 16-20 June 2003, Published by Keldysh Institute of Applied Mathematics, Space Informatics Analytical Systems (KIA Systems), Moscow, Russia, pp. 56-76, 2003.
- Schildknecht T., et al., The Search for Debris in GEO, *Advances in Space Research*, Vol. 28, 1291-1299, 2001.
- Schildknecht T., et al., Optical Survey for Space Debris in GEO, in Bendisch J. (Ed.), *Space Debris 2001*, Sciences and Technology series, Vol. 105, Univelt Inc., San Diego, California, USA, pp. 9-21, 2002.
- Schildknecht T., et al., Optical Observations of Space Debris in GEO and in Highly-Eccentric Orbits, *Advances in Space Research*, Vol. 34, 901-911, 2004a.
- Schildknecht T., et al., Optical Observations of Space Debris in Highly Eccentric Orbits, Oral Presentation PEDAS1/B1.6-0007-04, Space Debris Session, 35<sup>th</sup> COSPAR Scientific Assembly, Paris, France, July 22, 2004b.